



Contents lists available at ScienceDirect

Journal of Wind Engineering & Industrial Aerodynamics

journal homepage: www.elsevier.com/locate/jweia

An improved $k-\omega$ turbulence model for the simulations of the wind turbine wakes in a neutral atmospheric boundary layer flow

Ioannis Bouras, Lin Ma^{*}, Derek Ingham, Mohamed Pourkashanian

Energy 2050, Faculty of Engineering, The University of Sheffield, S10 2TN, England, UK

A B S T R A C T

Correct prediction of the recovery of wind turbine wakes in terms of the wind velocity and turbulence downstream of the turbine is of paramount importance for the accurate simulations of turbine interactions, overall wind farm energy output and the impact to the facilities downstream of the wind farm. Conventional turbulence models often result in an unrealistic recovery of the wind velocity and turbulence downstream of the turbine. In this paper, a modified $k-\omega$ turbulence model has been proposed together with conditions for achieving a zero streamwise gradient for all the fluid flow variables in neutral atmospheric flows. The new model has been implemented in the simulation of the wakes of two different wind turbines and the commonly used actuator disk model has been employed to represent the turbine rotors. The model has been tested for different wind speeds and turbulence levels. The comparison of the computational results shows good agreement with the available experimental data, in both near and far wake regions for all the modeled wind turbines. A zero streamwise gradient has been maintained in the far wake region in terms of both wind speed and turbulence quantities.

1. Introduction

Large Eddy Simulation (LES), with the advances in computational power, is being more and more popular and is employed mainly in academia. Many researchers such as Goodfriend et al. (2015), Porte – Agel et al. (2011), Churchfield et al. (2012a,b) have employed LES to simulate successfully the neutral atmospheric boundary layer as well as the wind turbine wakes. However, despite the enormous advances in Computational Fluid Dynamics (CFD) techniques in recent years, RANS simulations still dominate the simulations in many engineering applications, especially in industry.

Accurate simulations of the atmospheric boundary layer (ABL) flows is still a challenge, in particular when the focus is on the flow over manmade structures such as wind turbines, where large differences in the length scales are considered. The difficulty in simulating a homogeneous ABL with RANS has been widely reported (Richards and Hoxey, 1993; Blocken et al., 2007; Franke et al., 2007; Hargreaves and Wright, 2007; Yang et al., 2009; O'Sullivan et al., 2011; Yan et al., 2016). Since the ABL can be as high as 1 km and there is no boundary in the streamwise and spanwise directions, in the computational modeling of the flow over a structure, e.g. a wind turbine, reasonable distances from the region of interest have to be taken in order to reduce the computational time and efforts, and assumptions in the conditions at the boundaries of the computational domain have to be made which can be inconsistent with the physics of the ABL flow. As a result, when the RANS approach is

employed with conventional turbulence models, undesirable streamwise gradients of the primitive variables and turbulence quantities occur primarily due to the inconsistencies in the turbulence model with the boundary conditions employed.

In order to satisfy the flow conditions of a neutrally stratified ABL, the upstream and downstream boundaries of the computational domain should be assumed to have the same flow characteristics regarding the ground roughness and friction velocity, so that the ABL is fully developed at the downstream boundary and consistent with the prescribed inlet flow conditions. Any streamwise gradient of any variable is undesirable when compared to the flow conditions at the upstream and downstream boundaries. For the upper boundary of the computational domain, since the wind flow is driven by geostrophic winds, the imposition of a zero stress boundary condition at the upper boundary of the solution computational domain is not, theoretically, an appropriate choice.

Richards and Hoxey (1993) proposed a shear stress boundary condition together with a set of inlet flow profiles and they successfully simulated the neutral ABL without any undesirable streamwise gradients in their solutions. Their model is mathematically consistent, and the implementation of this model in the commercial CFD software ANSYS CFX and FLUENT by Hargreaves and Wright (2007) was successful in achieving a zero streamwise gradient by slightly modifying the standard grain sand rough wall function and the inclusion of a momentum source on the upper layer of cells of the computational domain. Furthermore, Blocken et al. (2007) have suggested 4 basic requirements for the

^{*} Corresponding author.

E-mail address: lin.ma@sheffield.ac.uk (L. Ma).

<https://doi.org/10.1016/j.jweia.2018.06.013>

Received 25 February 2018; Received in revised form 11 May 2018; Accepted 21 June 2018

homogeneity of the ABL and proposed some remedial measures to mitigate the problem with the inconsistency of the inlet profiles with the wall functions employed in the commercial CFD software FLUENT and CFX. Also, they used essentially a Dirichlet boundary condition at the upper boundary of the solution domain by directly specifying the values of the velocity and turbulence. This method recovers, to some extent, the desirable profiles of the velocity and turbulence quantities but it has the drawback that it does not allow mass to enter or exit the upper boundary (O'Sullivan et al., 2011) which is not ideal. Yang et al. (2009) used a dissipating profile for the turbulent kinetic energy with the height based on laboratory experimental data and they implemented them in the commercial CFD software FLUENT and their computational results have shown good agreement with their experimental data. Parente et al. (2011) modified the standard $k - \epsilon$ turbulence model by adding source terms for the turbulent kinetic energy and turbulent dissipation rate to allow flexibility on the imposed profiles as in the Richards and Hoxey approach of a steady value for the turbulent kinetic energy was a rough approximation of the neutral ABL (Richards and Norris, 2015). O'Sullivan et al. (2011) performed an error analysis on the profiles of the velocity magnitude, turbulent kinetic energy and eddy dissipation rate which are produced by the inconsistent boundary conditions employed and they proposed an extension to the shear stress boundary condition on the upper boundary of the domain based on the profiles for turbulent kinetic energy and eddy dissipation rate generated by Yang et al. (2009). Their results showed improvement by minimizing any streamwise gradients for both Yang et al. (2009) and Richards and Hoxey (1993) profiles and proven that regardless of the type of the boundary condition at the upper boundary the increased height of the computational domain can decrease the errors.

The importance of accurate predictions of the homogeneous ABL is related to with various applications, such as pollutant dispersion and meteorological models (Mokhtarzadeh Dehghan et al., 2012; Juretic and Kozmar, 2013). By summarizing various papers, Tominaga et al. (2008) made some recommendations for the simulations of flows around buildings regarding the inlet conditions, the turbulence models, the boundary conditions, as well as the appropriate domain size, while the type of the zero streamwise gradient condition does not appear to play any role due to the strong velocity gradients and consequently, high turbulence generation.

Research on achieving the streamwise gradient condition for the simulations of the wind turbine wakes has not been fully investigated. The importance of the zero streamwise gradient condition, along with the correct recovery in the very far wake region, for the simulation of the wind farms, is of paramount importance. This is because the velocity and turbulence of the first turbine become the inlet for the turbines at the rear of the first turbine. Consequently, failure in achieving the streamwise gradient condition, depending on the consistency of the employed model with the inlet values and boundary conditions, may have disastrous consequences in the predicted power output of the wind farm as well as in the structural damage of the wind turbines.

There are many researchers who have noticed the problems of modeling flow and turbulence behind the wind turbines. Prospathopoulos et al. (2010) modeled 2 wind farms, one on a flat terrain and another on a complex terrain for various wind directions, in neutral atmospheric conditions, using the actuator disk approach. They applied the $k - \omega$ turbulence model with the Boussinesq eddy viscosity assumption, as well as another definition of the eddy viscosity, which is based on the Durbin correction (1996), to show the differences in the power production with the conventional and the modified definition of the eddy viscosity for both types of terrain. Cabezón et al. (2010) simulated a 43 wind turbine wind farm on a complex terrain with the wake model CFDWake 1.0 in order to validate and compare their results with the available experimental data. Makridis and Chick (2013) used the guidelines of Blocken et al. (2007) to simulate a wind turbine with the actuator disk model over a complex terrain as well as a small coastal wind farm and compared their results with experimental data. They used the

commercial CFD software FLUENT and in order to take into account the anisotropy of the atmospheric turbulence, they used the RSM model. Castellani and Vignaroli (2013) also applied the actuator disk technique for a small wind turbine using the CFD code Phoenics and the comparison of their results with the available experimental data was generally good, however, no discussion was presented on the zero streamwise gradient condition. Simisioglou et al. (2016) modeled various large horizontal axis wind turbines using the commercial CFD software PHOENICS. They made a few parametric studies based on the convergence criteria, the turbulence model, the grid resolution and the actuator disk thickness. They validated their results with the thrust and power curve for one of the turbines they used. However, in the absence of experimental data for the wake region, they used results from large eddy simulations for validation. Similarly to Makridis and Chick (2013), Nedjari et al. (2017) examined the actuator disk model with the standard $k - \epsilon$ model on a flat and a complex terrain and validated their results with experimental data. The validation of the model with experimental data was very good in the near or far wake region, however in the very far wake region the normalized velocity appears to recover to approximately 85% of the inlet velocity and remains at this value until the outlet. Also, no results for the turbulent kinetic energy were shown. It is characteristic that none of the above researchers performed any simulations of an empty domain in order to show the changes of their inlet conditions on the velocity, turbulent kinetic energy and eddy dissipation rate within the domain.

Many researchers, such as Kasmi and Masson (2008) and Simisioglou et al. (2016) have shown that 2 equation turbulence models fail to predict the velocity and turbulence quantities in the near or the far wake regions of the wind turbine. Kasmi and Masson (2008) proposed a remedy to this problem by adding a source term in the region of the turbine in the equation for the eddy dissipation of the standard $k - \epsilon$ model, based on the work done by Chen and Kim (1987). Their proposed model showed significant improvement in predicting the velocity downstream of the turbine over the standard $k - \epsilon$ model when comparing their results with experimental data for 3 wind turbines, however, no quantification of their results has been reported. Recently, El - Askary et al. (2017) have implemented Kasmi and Masson (2008) model and achieved some improvement of the results when compared to experimental results. This can partially be explained by the fact that Kasmi and Masson (2008) have also included the nacelle in their simulations while El - Askary et al. (2017) have not included it. Also, Kasmi and Masson (2008) added 2 extra terms in the transport equations of the $k - \epsilon$ equation while El - Askary et al. (2017) have not used them. However, these 2 extra terms in the transport equations of the $k - \epsilon$ model violate the zero streamwise gradient condition. Finally, Kasmi and Masson (2008) simulated 3 different wind turbines but with the same relative inlet turbulence levels, and therefore it is unknown how their model will perform for different relative inlet turbulence levels.

The standard $k - \epsilon$ model has the theoretical advantage of being suitable for free shear fully turbulent flows, which is the case for this application, so it is the most obvious model to use. However, one of its most important weaknesses is its lack of sensitivity to adverse pressure gradients (Menter, 1994). On the other hand, the standard $k - \omega$ model is suitable for wall bounded flows and for flows where adverse pressure gradients occur. Although there are no strong adverse pressure gradients involved for the wind turbine wakes, there is a small increase in the pressure upstream and downstream of the turbine at the hub - height, a fact which makes the standard $k - \omega$ model, theoretically, the optimal solution for this application. Finally, the modification of Chen and Kim (1987), which is employed around the wind turbine in the Kasmi and Masson (2008) model, is highly dependent on the relative turbulent kinetic energy of the field in the standard $k - \epsilon$ model, while in the standard $k - \omega$ model is independent. Details are presented later in theory section.

In this paper, the 3D Reynolds Averaged Navier - Stokes equations are solved with the standard $k - \omega$ turbulence model to examine an empty domain for a neutrally stratified atmospheric boundary layer. An equation for the zero streamwise gradient condition is proposed by solving the

transport equations for the standard $k - \omega$ model, and simulations have been performed for various turbulence levels. Validation of the results is based on theoretical values for a neutral atmosphere proposed by Richards and Hoxey (1993). Then, the model is applied to the simulations of wind turbine wakes with a small modification in the transport equation of the specific dissipation rate based on the work performed by Chen and Kim (1987) in the region around the wind turbine. The rotor of the wind turbine is modeled using the actuator disk approach based on the blade element theory and 2 small wind turbines are simulated for various inlet velocity and turbulence levels. The model performs well in both near and far wake regions and the properties of the neutral atmosphere are recovered to the undisturbed inlet conditions far away downstream of the wind turbine. The simulations were performed with the commercial CFD software FLUENT and the grid generation in the software ICEM.

2. Modifications to the standard $k - \omega$ model

For a neutral atmospheric boundary layer flow, the following assumptions can be made for a flat empty computational domain, see Richards and Hoxey (1993):

- (a) The vertical velocity is zero throughout the domain
- (b) The pressure is constant throughout the domain
- (c) The shear stress is constant throughout the domain, being independent of the height and it is given by:

$$\tau_0 = \rho u_*^2 \tag{1}$$

where ρ is the density of the air, which is considered as a constant throughout the atmospheric boundary layer and u_* is the friction velocity.

The profiles for the velocity, turbulent kinetic energy and eddy dissipation rate, respectively are as follows:

$$U_{(y)} = \frac{u_*}{\kappa} \ln \left(\frac{y + y_0}{y_0} \right) \tag{2}$$

$$k = \frac{u_*^2}{\sqrt{C_\mu}} \tag{3}$$

$$\varepsilon_{(y)} = \frac{u_*^3}{\kappa(y + y_0)} \tag{4}$$

where $U_{(y)}$ and $\varepsilon_{(y)}$ is the velocity magnitude and the eddy dissipation rate, respectively, as a function of the height, y_0 is the roughness length of the ground and κ is the von Karman constant. k is the turbulent kinetic energy.

The assumption of a constant value of the turbulent kinetic energy throughout the domain has been criticized by some researchers, such as Yang et al. (2009), Parente et al. (2011) and Richards and Norris (2015). However, the turbulent kinetic energy appears to have an almost steady value for the first 100 m within the ABL (Juretic and Kozmar, 2013), and it dissipates further away with the height and reaches a value of approximately 5% of the value that it has close to the ground at the height of the ABL (Allaers and Meyers, 2015). Also, most researchers, such as Kasmi and Masson (2008), Prospathopoulos et al. (2010), Cabezon et al. (2010), Makridis and Chick (2013) and Simisioglou et al. (2016) used a steady value for the turbulent kinetic energy at the inlet of the domains in order to simulate the wake region around a wind turbine with the actuator disk model. The assumption of a constant value of the turbulent kinetic energy is a good approximation for the simulations of small wind turbine wakes since, in many cases, for economic issues, experimental data are measured only at the hub – height at various locations upstream or downstream of the turbine, although, as explained earlier, it is not consistent with the neutral ABL.

Richards and Hoxey (1993) discovered a condition for the standard k

– ε model that satisfies equation (2)–(4). In a similar way, a condition for the elimination of the streamwise gradients for any variable in the standard $k - \omega$ (Wilcox, 1988) model can be found.

The formulation of the standard $k - \omega$ model (Wilcox, 1988) is given as follows (see FLUENT Theory Guide (2011)):

$$\frac{\partial}{\partial t}(\rho k) + \frac{\partial}{\partial x_i}(\rho k u_i) = \frac{\partial}{\partial x_i} \left[\left(\mu + \frac{\mu_t}{\sigma_k} \right) \frac{\partial k}{\partial x_i} \right] + G_k - Y_k + S_k \tag{5}$$

$$\frac{\partial}{\partial t}(\rho \omega) + \frac{\partial}{\partial x_i}(\rho \omega u_i) = \frac{\partial}{\partial x_i} \left[\left(\mu + \frac{\mu_t}{\sigma_\omega} \right) \frac{\partial \omega}{\partial x_i} \right] + G_\omega - Y_\omega + S_\omega \tag{6}$$

The eddy viscosity is defined as:

$$\mu_t = a^* \frac{\rho k}{\omega} \tag{7}$$

where

$$a^* = a_\infty^* \left(\frac{\beta_i}{3} + \frac{\rho k}{6} \right) \left(1 + \frac{\rho k}{6} \right) \tag{8}$$

equations (5) and (6), on taking into account the fact that the flow in an empty domain is essentially one dimensional and time independent, there are no buoyancy or compressibility effects, and the turbulent kinetic energy is constant for any direction within the domain, may be simplified as follows:

$$0 = G_k - Y_k \tag{9}$$

$$0 = \frac{\partial}{\partial y} \left[\left(\mu_t + \frac{\mu_t}{\sigma_k} \right) \frac{\partial k}{\partial y} \right] + G_\omega - Y_\omega \tag{10}$$

Finally, the connection between the eddy dissipation rate and the specific dissipation rate (or eddy frequency) is given by (Wilcox, 1988):

$$\omega = \frac{\varepsilon}{k \beta_\infty^*} \tag{11}$$

By making some mathematical calculations, it can be easily concluded that equation (2)–(4) satisfy automatically equation (5) but satisfy equation (6) only if the following expression is satisfied:

$$\frac{1}{\sigma_\omega \sqrt{\beta_\infty^*}} + \frac{1}{\kappa^2} = \frac{\beta_i}{\beta_\infty^* \kappa^2} \tag{12}$$

Therefore, to achieve a zero streamwise gradient, equation (12) must be satisfied and it is independent of the friction velocity, the height of the domain or the roughness of the ground, in a similar way as that is employed in the standard $k - \varepsilon$ model (Richards and Hoxey, 1993).

The constant β_∞^* is defined by the existent turbulence levels in the field (equation (3)). Instead of the coefficient C_μ that the standard $k - \varepsilon$ model uses, the turbulence levels for the standard $k - \omega$ model are defined by:

$$k = \frac{u_*^2}{\sqrt{\beta_\infty^*}} \tag{13}$$

Consequently, for specific turbulence levels, which are defined by the coefficient β_∞^* , the constants σ_ω and β_i have to be chosen accordingly in order to satisfy the expression (12) in order to avoid streamwise gradients for any variable within the solution domain.

Finally, the following consideration was taken in order to conclude to the expression (12):

$$\mu_l \ll \mu_t \tag{14}$$

i.e. the laminar viscosity was omitted from the transport equations for

turbulent kinetic energy and specific dissipation rate. The error in using this simplification is expected to be negligible since the flow is highly turbulent.

As discussed previously, since 2 equation turbulence models fail to predict the velocity and turbulence quantities in the near or the far wake regions of the turbine, [Kasmi and Masson \(2008\)](#) proposed a remedy to this problem by adding a source term in the vicinity of the turbine in the equation for the eddy dissipation in the standard $k - \epsilon$ model, and this is based on the work performed by [Chen and Kim \(1987\)](#). This source term is described by the following formula:

$$S_\epsilon = C_{\epsilon 4} \frac{G_k}{\rho k} \quad (15)$$

The coefficient $C_{\epsilon 4}$ was set at the default value of 0.25. The main idea behind this source term is the fact that the equation for the eddy dissipation rate for the family of the $k - \epsilon$ models is empirical, and therefore there are many applications that the standard $k - \epsilon$ model fails to accurately predict the flow (e.g. the backward facing step, swirling flow problems etc.) and gives highly diffusive results. Therefore a second time scale (equation (15)) is added to the eddy dissipation equation to represent the energy transfer from the large to the small scales more effectively. In particular, the energy transfer from the large scales to the small ones is controlled by the production range scale and the dissipation rate time scale ([Chen and Kim, 1987](#)). Consequently, [Chen and Kim \(1987\)](#) added a second time scale in the eddy dissipation equation of the standard $k - \epsilon$ model and they found a significant improvement for a wide range of engineering applications.

Although this term was designated to be used in the family of $k - \epsilon$ models, it appears that it improves the results in the standard $k - \omega$ model as will be shown later. As [Kasmi and Masson \(2008\)](#) showed that the standard $k - \epsilon$ model overestimates the turbulent kinetic energy for the wind turbine wakes, the same applies for the standard $k - \omega$ model. This may be explained by the fact that [Wilcox \(2006\)](#) used a slightly different version of his initial $k - \omega$ model by adding a cross diffusion term in the specific dissipation rate equation along with a stress limiter modification to the definition of the eddy viscosity, as many researchers have shown improved results of this version.

The most important theoretical advantage of the $k - \omega$ model, in relation to the $k - \epsilon$ model, is that it does not include any constant in the definition of the eddy viscosity. In fact, in the standard $k - \epsilon$ model the production term (G_k) that is included in equation (15) includes the eddy viscosity which depends highly on the constant C_μ which defines the turbulence levels of the field. However, in the $k - \omega$ model there is no C_μ constant (or β_∞^* as the turbulent kinetic energy in the family of $k - \omega$ models is defined by the coefficient β_∞^* in the neutral atmosphere as described earlier) so the model is independent of the relative to the velocity turbulent kinetic energy.

3. Examination of the empty domain

In order to validate the modified $k - \omega$ model and check if the zero streamwise gradient of the fluid flow properties can be maintained, simulations have been performed for an ABL flow throughout an empty domain. The dimensions of the computational domain employed are 10,000 m, 405 m and 50 m in the x,y and z directions, respectively. The y direction refers to the height of the domain from the ground. The 10 km length of the domain has been selected in order to make sure that the flow will be fully developed within this long domain while the 405 m height has been selected because it is considered as an adequate height for the simulation of any small or medium size wind turbine. Finally, a very short distance in the spanwise direction was selected because there are no gradients for any variable in this direction. A velocity inlet boundary condition was imposed at the inlet of the domain based on equation (2)–(4). The friction velocity of the wind flow is $u_* = 0.46 \text{ m/s}$ and the roughness length is 0.05 m, which is valid for a relatively low

roughness terrain. A value of $\beta_\infty^* = 0.033$ is used to define the turbulence levels at the inlet of the domain based on [Panofsky and Dutton \(1984\)](#) as well as other researchers, such as [Makridis and Chick \(2013\)](#) and [Kasmi and Masson \(2008\)](#). Regarding the rest boundary conditions, a pressure outlet boundary was imposed at the outlet, a symmetry (or zero gradients) at the lateral sides of the domain and a Dirichlet boundary condition at the upper boundary based on equation (2)–(4).

The third order MUSCL scheme was used for the discretization of the momentum equations and the second – order upwind scheme for the transport equations for the turbulent kinetic energy and specific dissipation rate and the SIMPLE algorithm was implemented for the pressure velocity coupling, while the convergence criteria were set to 10^{-7} for all the equations and this was found to be small enough to obtain graphically indistinguishable results. Mass imbalance has also been checked to make sure that all simulations have converged. Finally, regarding the grid resolution, 3 different grid sizes have been employed consisting of approximately 200,000, 600,000 and 1,800,000 elements. The numerical grids were fully structured and the refinement of the grid has been equally done in all directions.

[Fig. 1](#) compares the solutions for the velocity, turbulent kinetic energy and specific dissipation rate, respectively, for an empty domain at the inlet and outlet of the domain with various different grid sizes. Due to the rapid change of the eddy frequency with the height, the logarithmic scale is used in [Fig. 1 \(c\)](#), as well as in the contour map in [Fig. 2 \(c\)](#). An error analysis showed that the difference between the inlet and outlet for the turbulent kinetic energy is approximately 2% on the ground, for any grid size and it decreases with the height. [Fig. 2](#) illustrates contour maps of the velocity, turbulent kinetic energy and eddy frequency to show the development of these variables within the domain. The height of the domain was scaled up 4 times due to its initial small perpendicular to the ground direction, in relation to the length of the domain. A similar situation exists for the eddy frequency where the error appears to reach an error of approximately 4% close to the ground and it becomes gradually smaller with the height. Finally, regarding the velocity, it appears to have an error of approximately 2% close to the ground but it becomes less than 1% within the first 10 m from the ground. There are 2 reasons for the errors close to the ground for any variable. The first reason is due to the wall formulation which is not consistent with the profiles of equation (2)–(4) and it appears that the calculation of the turbulence quantities is a function of the friction velocity ([ANSYS FLUENT, 2011](#)). Another reason is attributed to the assumption of the negligence of the laminar viscosity (equation (14)) which is not valid on the ground. However, the differences are in general small, and it can be concluded that the velocity, turbulent kinetic energy and specific dissipation rate are maintained from the inlet to the outlet of the domain with a good accuracy. Moreover, parametric studies based on the friction velocity from 0.4 to 0.62 m/s and turbulence levels for values of β_∞^* from 0.033 to 0.1 showed small dependence and the comparison of the results with the theoretical values based on equation (2)–(4) was similar to the ones present in [Fig. 1](#). The small errors far away from the ground are attributed to the simplifications that have been made in theory, numerical and convergence issues. Finally, the results show negligible sensitivity to the grid size and this is due to the simplicity of the geometry. In particular, the maximum differences between the coarse and medium sized grid for the velocity, turbulent kinetic energy and eddy frequency were 0.12%, 0.16% and 0.72%, while the maximum differences in the same variables between the medium sized grid and fine grid were 0.06%, 0.11% and 0.57%, respectively, and consequently the numerical grid consisting of 600,000 elements has been used.

Most researchers who studied the characteristics of wind turbine wakes did not examine the zero streamwise gradient condition. It appears, although it has not been proven, that it is not important when a single turbine is examined due to the fact that the undisturbed wind conditions do not change significantly within a few characteristic lengths of the domain when the zero streamwise gradient condition is not

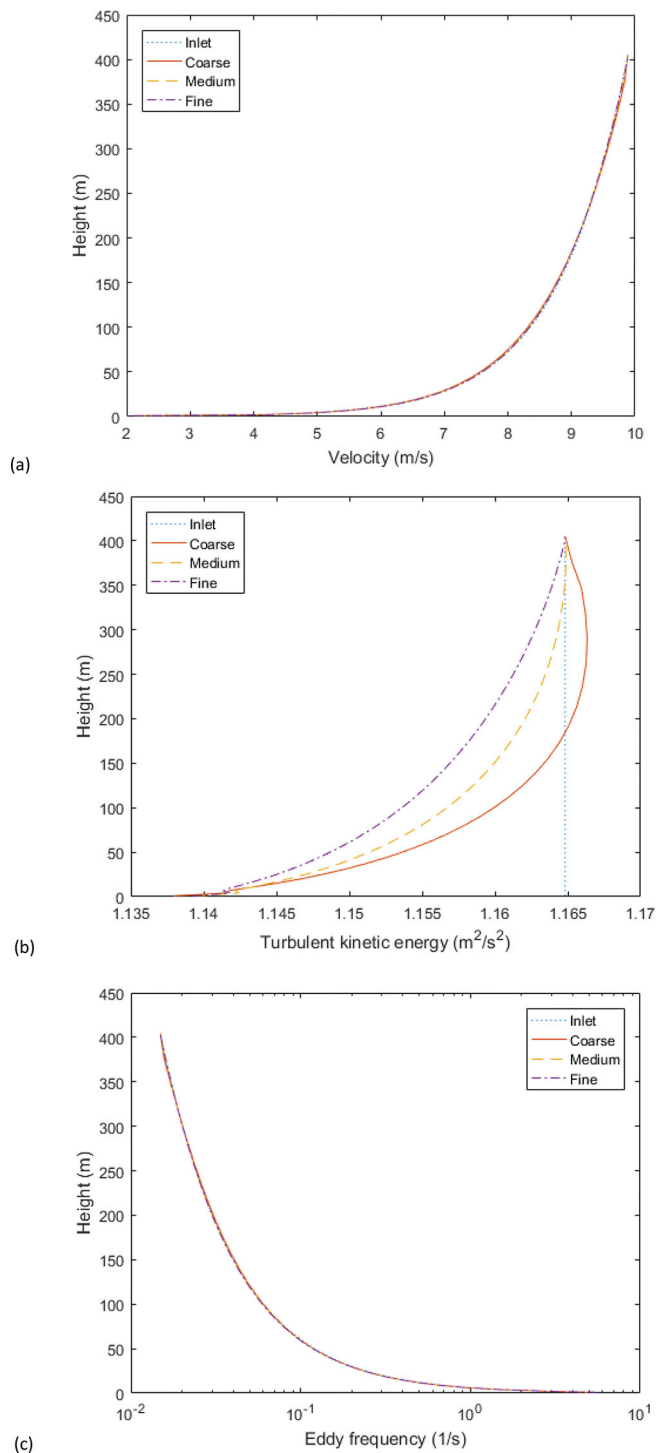


Fig. 1. Comparison of (a) velocity, (b) turbulent kinetic energy, and (c) specific dissipation rate between the inlet and outlet in a 10 km domain for 3 different grid sizes.

satisfied. However, when a large domain is examined with multiple wind turbines in any arrangement, it is of paramount importance that the velocity and turbulence levels have a correct recovery and, in the long run, recover to the undisturbed inlet conditions and be maintained as happens in nature.

In the next section, 2 different small wind turbines are examined and the importance of the zero streamwise gradient for all variables is illustrated.

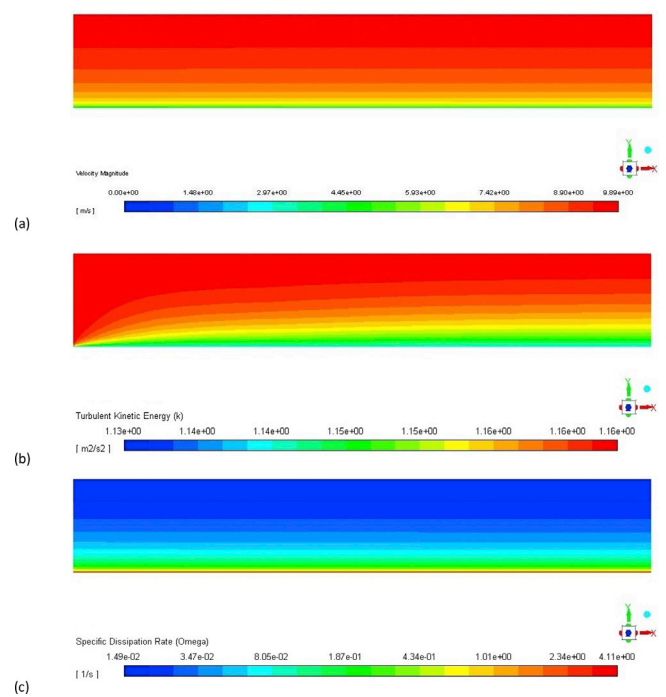


Fig. 2. Results of (a) velocity, (b) turbulent kinetic energy and (c) eddy frequency along the domain.

4. Modeling of a single wind turbine using the actuator disk theory

A full – scale detailed aerodynamic simulation of a wind turbine is very time consuming since it requires a transient simulation as well as a very refined numerical grid around the blades, the nacelle, the tower of the wind turbine etc. Consequently, many other computationally cheaper ways of simulating the wind turbine wakes have been developed. The simplest model is the actuator disk model without rotation and is based on the blade element method.

Mikkelsen (2003) has analyzed many models for the modeling of the rotor of the wind turbines. The simplest of all models, when the aerodynamics of the wind turbine is unknown, is the actuator disk model without rotation and based on the thrust coefficient (C_T) of the turbine. The pressure drop through the wind turbine can be calculated by the following equation:

$$\Delta P = 0.5\rho AC_T U_\infty^2 \tag{16}$$

where A is the rotor disk area and U_∞ is the undisturbed wind velocity upstream of the turbine. The only information that is needed is the thrust coefficient and the diameter of the wind turbine.

4.1. Nibe – B 630kw turbine

The first wind turbine that is examined is a Nibe – B 630kw turbine and this is a horizontal 3 bladed wind turbine operating at 33 rpm with a 40 m diameter at 45 m hub – height. In the simulations performed in this paper, the actuator disk model without rotational effects was employed.

Regarding the size of the computational domain, the distance from the inlet to the turbine is $4D$, the distance from the turbine to the outlet is $40D$, the distance from the turbine to the upper boundary is $5D$ and the distance between the turbine and the lateral sides of the domain is $4D$, where D is the diameter of the wind turbine. The boundary conditions were the same as in the empty domain examined earlier along with the other settings of the solver. The pressure drop along the wind turbine was calculated from equation (16).

As stated in theory, condition (12) must be satisfied in order to ensure the recovery of the velocity and turbulence quantities in the far wake region. The zero streamwise gradient condition is important in the far wake region, however, the recovery of the velocity and turbulence are highly sensitive on the σ_ω coefficient. By performing some parametric studies, a value of $\sigma_\omega = 1.3$ was chosen as the optimum coefficient for all wind turbines. Given a coefficient of $\beta_\infty^* = 0.033$ for the definition of the turbulence levels and a value of $\sigma_\omega = 1.3$, the value of $\beta_1 = 0.0575$ satisfies equation (12). The Von Karman constant that is used is $\kappa = 0.4187$. The standard $k - \omega$ model also has been employed to illustrate the differences between the 2 models against the experimental data. The only modification that has been done to the standard $k - \omega$ model is the coefficient β_∞^* and it has been given the same value as in the modified $k - \omega$ model in order to match the inlet turbulent kinetic energy at the inlet of the domain (equation (12)).

A grid independence study has been carried out. Given the simplicity of the geometry, the requirement of the simulation regarding its number of cells was not very demanding. 3 different grid sizes have been simulated consisting of approximately 140,000, 600,000 and 1,560,000 cells. All of them were fully structured numerical grids and the refinement from the coarse to the fine grid has been done everywhere in the domain but mainly in the region around the wind turbine and at a few characteristic lengths upstream and downstream of it. The maximum difference between the 2 coarser numerical grids was found to be approximately 2.5% for the velocity and 3.5% for the turbulent kinetic energy, while the maximum difference in the results obtained using the 2 finer grids were less than 0.2% for the velocity and less than 0.5% for the turbulent kinetic energy. Consequently, the numerical grid consisting of 600,000 elements was employed and a similar grid has been created with a similar number of cells and spacing between the nodes for the second wind turbine that is examined later.

It should be noted that the near wake region is considered as the region within 3D at the rear of the turbine, the far wake region as the region within 5.5D and 8D at the rear of the turbine and the very far wake region as the region from 8D up to the outlet.

Fig. 3 illustrates the predicted normalized velocity and turbulence intensity in comparison to experimental data and the standard $k - \omega$ model for $U_{hub} = 8.5m/s$, $C_T = 0.82$ and $Tl_{hub} = 11\%$ along the centerline at the hub height of the turbine. This is the condition when the turbine is operating at 630kw. The velocity is normalized with the inlet velocity value and the experimental data are provided by Taylor et al. (1985).

It is observed in the far wake region that the modified $k - \omega$ model is able capture the correct turbulence levels, according to the experimental data. Also, in the very far wake region, close to the outlet boundary, the turbulence levels drop to the undisturbed values that are applied at the inlet boundary. It is interesting that the highest value of the turbulent kinetic energy does not appear in the near wake region of the turbine but, rather, a few characteristic lengths downstream of the turbine ($\approx 4D$). This observation is also visible in other experimental data for the second wind turbine that is presented later. This trend of the turbulence intensity is captured by the modified $k - \omega$ model, while the standard $k - \omega$ model failed to capture the turbulent kinetic energy anywhere within the domain.

The velocity also shows a similar trend to the turbulent kinetic energy. At the near wake region (2.5D) the modified $k - \omega$ model closely predicted the wind velocity, and in the far wake region the velocity is predicted very well, while the standard $k - \omega$ model failed to predict the velocity anywhere within the domain. It is also noticeable that the velocity and turbulent kinetic energy did not converge to the undisturbed inlet values according to the standard $k - \omega$ model, which was expected since it does not satisfy equation (12). These results are indicative of the very simplistic model that is used to simulate the wind turbine. A more accurate or elaborative model, instead of the actuator disk model without rotational effects based on the thrust coefficient, would have given more

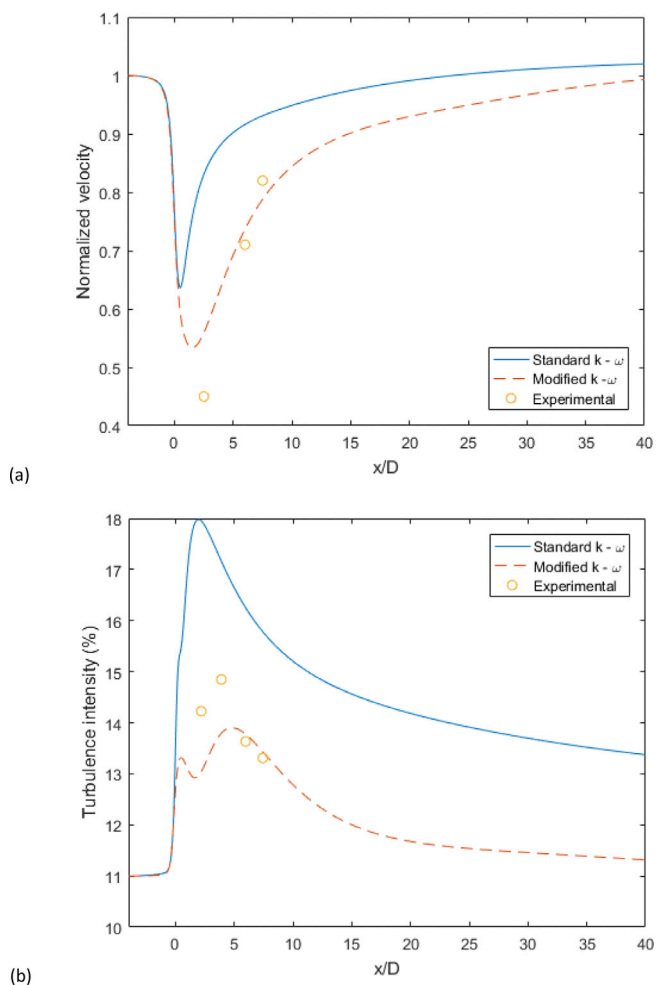


Fig. 3. (a) Normalized velocity and (b) turbulence intensity along the streamwise direction at the hub – height of the domain.

accurate predictions for the velocity in the near wake region.

According to the original source of the experimental data, the mast located 7.5D downstream of the turbine was not aligned exactly with the wind direction (Taylor et al., 1985). This statement can be seen from the almost linear behavior, if these 3 points are connected, of the velocity according to the measurements. Also, as will be shown later, the velocity of the wind does not have such a steep recovery for other wind turbines, or even for the same turbine under different operational conditions.

As far as the errors are concerned, the difference of the velocity in the near wake region with experimental data was more than 20% while in the far wake region this reduced to less than 5%, and the difference in the turbulence intensity was less than 10% in the near or far wake region.

Fig. 4 shows the turbulence intensity perpendicular to the ground from the hub – height up to 1.2D above the centerline of the hub – height of the turbine located at 2.5D at the rear of the turbine. There appears to be a peak in the turbulence intensity at 0.5D and probably this arises from the tip of the turbine blades. The modified $k - \omega$ model is able to capture this increase in the turbulence in this region but it fails to predict the magnitude of it, which is indicative of the very simplistic model that is used to simulate the wind turbine. Another explanation may lie to the fact that the pressure drop that has been applied on the disk is based on the undisturbed velocity value at the hub – height of the turbine. However, the undisturbed velocity changes with the height based on the logarithmic velocity profile as given equation (6). Consequently, a higher pressure drop from the hub – height up to the tip of the turbine would, theoretically, give higher turbulence levels. Another interesting fact is that the measured turbulence intensity drops less than 10% while the

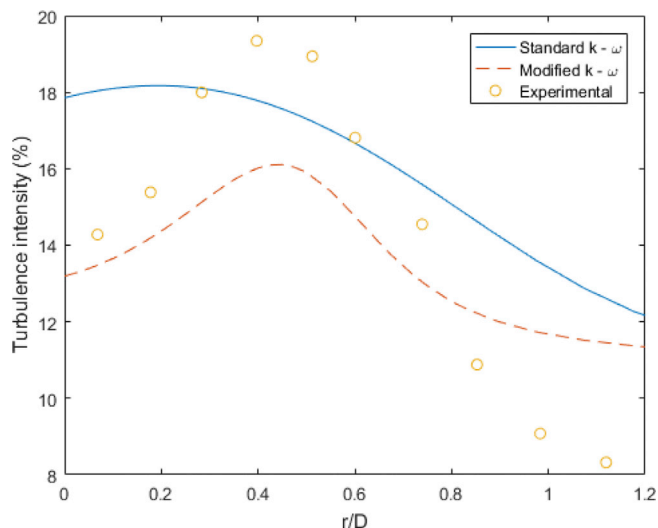


Fig. 4. Turbulence intensity distribution along a line perpendicular to the ground from the hub – height up to 1.2D placed at 2.5D at the rear of the turbine.

inlet turbulence intensity is 11%. The only possible explanation could be that the turbulent kinetic energy slightly decreases with the height of the domain, although nothing is stated about this in the report. In any case, as stated in the introduction, employing a constant turbulent kinetic energy at the inlet may be a special or a simplified case, however, it approximates the neutral atmospheric conditions and it has been the view of many researchers for the simulation of small wind turbines (Kasmi and Masson, 2008; Makridis and Chick, 2013).

Taking into account the fact that the turbulence generation depends on the velocity gradients in the 2 equation turbulence models based on the Boussinesq assumption for isotropy, it can be concluded that a more elaborative model for the wind turbine, e.g. the inclusion of the nacelle and the tower, would have given even better results for both the velocity and turbulence because the minimum velocity would have been lower, and consequently, the turbulence levels in the near wake region would have been larger, due to the higher pressure drop imposed at the disk.

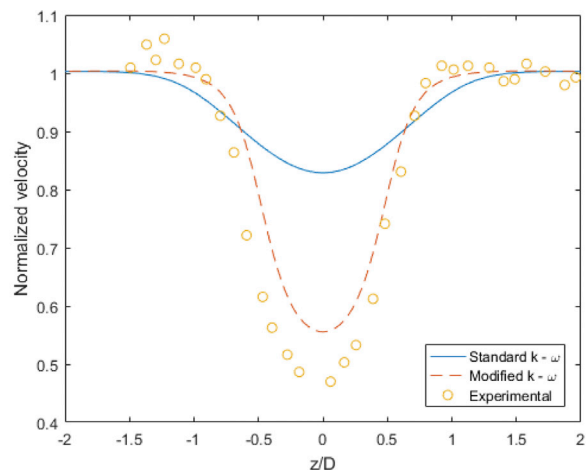
Fig. 5 illustrates the normalized velocity distribution from one lateral side to the other of the domain at the hub – height located at (a) 2.5D, (b) 6D and (c) 7.5D at the rear of the turbine.

The modified $k - \omega$ model in the far wake region at 6D and 7.5D at the rear of the turbine predicts the velocity very well although the width of the velocity deficit is larger according to the experimental data at a distance of 6D at the rear of the turbine. In the region 7.5D downstream of the turbine the velocity appears to be slightly underestimated, however, as stated earlier, the actual velocity is lower than the values that appear in Fig. 5 because the mast was not 100% aligned with the wind turbine. This statement is also enforced by the fact that the normalized velocity, according to the experimental data appears to be higher than 1 close to the lateral sides of the domain. If the computationally predicted results had been normalized with a lower value, the validation would have been even better.

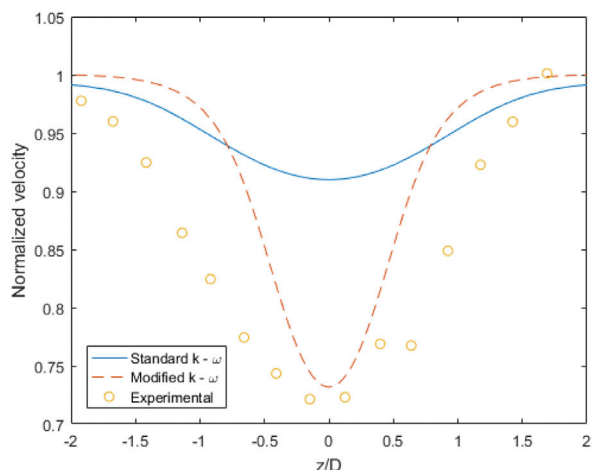
Figs. 6 and 7 illustrate the normalized velocity from one lateral side of the domain to the other lateral side at the hub – height at (a) 2.5D, (b) 6D and (c) 7.5D for the same turbine but for different wind velocity and turbulence levels. Fig. 6 shows the normalized velocity for $U_{\infty, hub} = 9.56\text{m/s}$, $TI = 11\%$ and $C_T = 0.77$ and Fig. 7 shows the normalized velocity for $U_{\infty, hub} = 11.52\text{m/s}$, $TI = 10.5\%$ and $C_T = 0.67$.

The results for $U_{\infty, hub} = 9.56\text{m/s}$ and $U_{\infty, hub} = 11.526\text{m/s}$ have a similar behavior to the results presented in Fig. 4 for $U_{\infty, hub} = 8.5\text{m/s}$.

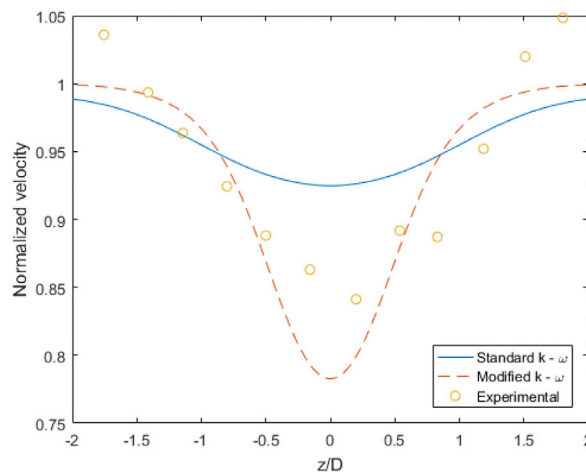
In general, the modified $k - \omega$ model predicts well the velocity at 6D and 7.5D at the rear of the turbine while it rather overestimates the velocity 2.5D at the rear of the turbine, while the standard $k - \omega$ model



(a)



(b)

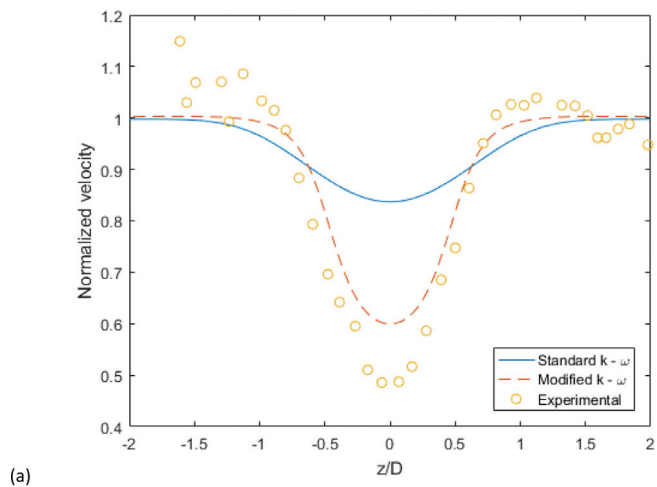


(c)

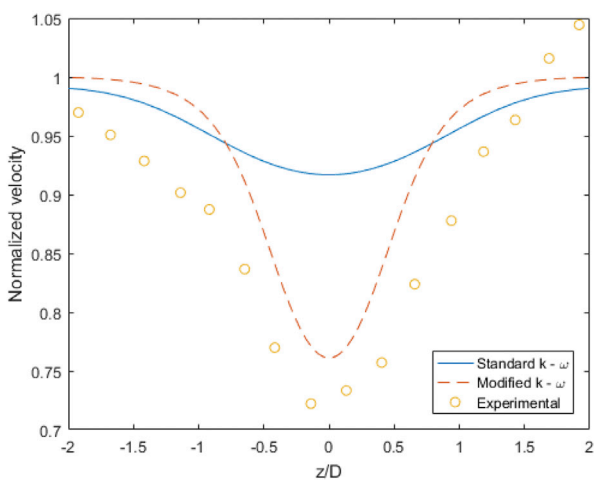
Fig. 5. Distribution of the normalized velocity along the lateral sides of the domain at the hub – height at (a) 2.5D, (b) 6D and (c) 7.5D.

failed to predict the velocity correctly anywhere within the domain. The problem with the normalized velocity being over 1 according to the measurements is still present for all inlet velocity values as seen in Figs. 5(c) and 6(c) and 7(c).

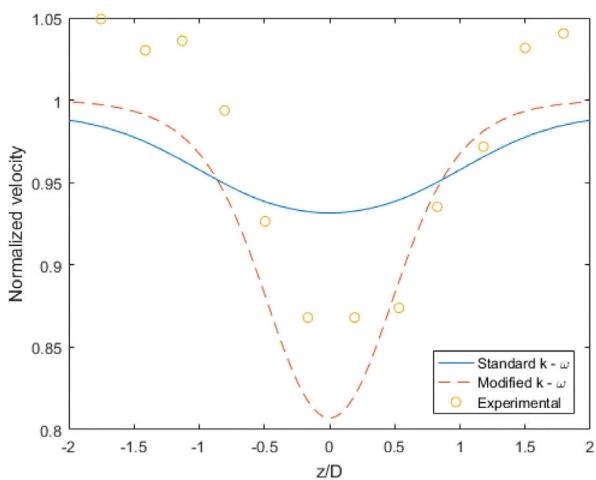
Also, it is observed from Figs. 5–7 that, as the undisturbed inlet



(a)



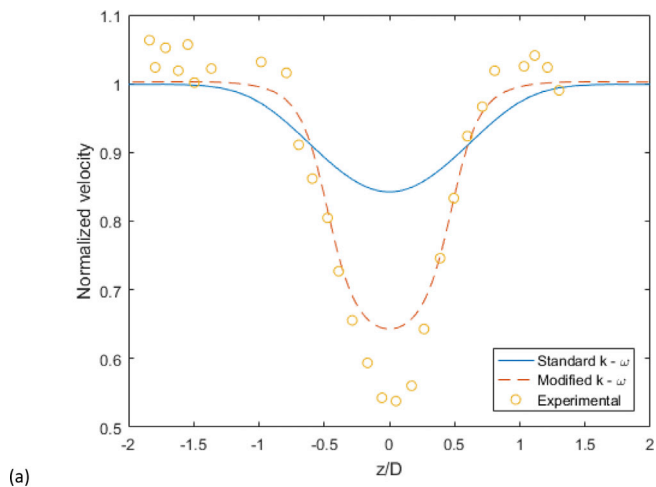
(b)



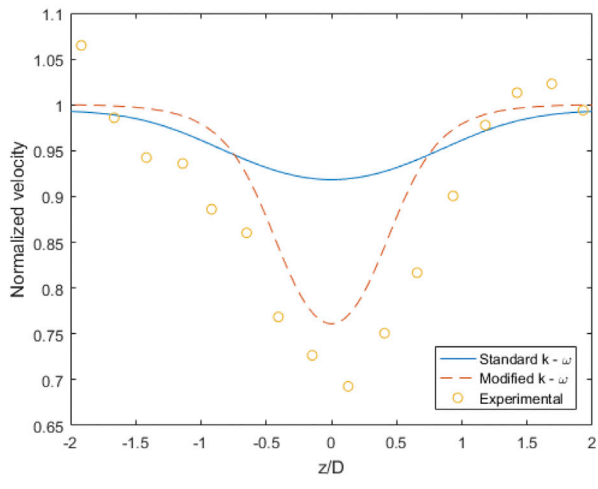
(c)

Fig. 6. Distribution of the normalized velocity along the lateral sides of the domain at the hub – height at (a) 2.5D, (b) 6D and (c) 7.5D for $U_{\infty,hub} = 9.56m/s$.

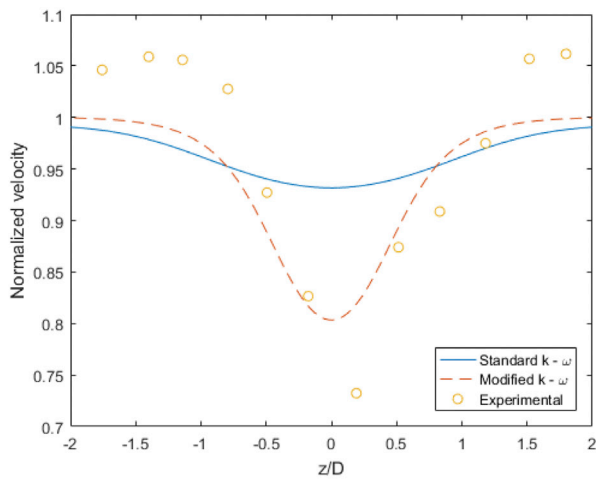
velocity decreases, the results close to the turbine become better when compared to experimental data, although the difference is generally small. The explanation for this behavior lies to the thrust coefficient. As stated earlier, the pressure drop that is applied on the disk is based on equation (16) and the model does not include any fixed parts of the wind



(a)



(b)



(c)

Fig. 7. Distribution of the normalized velocity along the lateral sides of the domain at the hub – height at (a) 2.5D, (b) 6D and (c) 7.5D for $U_{\infty,hub} = 11.52m/s$.

turbine such as the nacelle or the tower. The pressure drop of any fixed part of the turbine would have been calculated by the same formula, equation (16), but it would have included the drag coefficient instead of the thrust coefficient. However, as the velocity increases, the thrust coefficient, based on the power curve of the turbine, decreases, while the drag coefficient of the bluff bodies is not that sensitive to the inlet velocity, at least for fully turbulent flows, which is the case in the present

investigation. Taking into account the fact that the drag coefficient of the fixed parts of the turbine is higher than the thrust coefficient, and almost steady regardless of the velocity, it can be concluded that for low velocities, where the thrust coefficient is higher, the omission of the fixed parts of the turbine affects the results to a smaller extent than for the cases of the higher velocities. This statement will be validated later when the results of the Holec turbine are presented, although the difference is smaller due to the small differences in the thrust coefficient.

4.2. The Holec wind turbine

The second wind turbine that is examined is a small Holec horizontal axis three-bladed turbine with a rated power of approximately 300 kW. A wind farm of these turbines is located at Sexbierum, a village in northern Holland. The examination of another wind turbine is important in order to show the universality of the modified $k-\omega$ model and in order to show that the model is not sensitive to the inlet turbulence levels, and this is because the turbulence levels in this region are relatively low. The measurement data are taken from Cleijne (1992).

The computational setup is similar to the Nibe – B 630kw wind turbine explained previously. The flow conditions are based on Cleijne (1992). The logarithmic velocity profile is still valid, as in all atmospheric flows under neutral stratification within the surface layer where small wind turbines are located, but the turbulence levels are quite lower in relation to the previous wind turbine. However Cleijne (1992), is rather vague when it comes to the inlet turbulence levels. They took measurements at 3 different heights and analytically expressed the turbulence intensity and the corresponded roughness length, but in the results section for high yaw angles ($25^\circ - 30^\circ$) the turbulence levels appear to be far lower than the initially estimated ones for every mast. For this reason, the results for the turbulence intensity based on the results of the wind turbine for high angles of attack of the wind will be considered. In any case, the constant value for the turbulent kinetic energy, regardless of the height, appears to be almost valid based on all of their measurements.

The measured undisturbed normalized turbulent kinetic energy appears to be in the range 0.011–0.014. The normalization of the turbulence intensity was achieved with the squared undisturbed velocity inlet. These inlet turbulence levels correspond to a value of approximately $\beta_\infty^* = 0.09$ for the standard $k-\omega$ model, and consequently the standard $k-\omega$ model has been used without any modifications for the simulations. This value of β_∞^* gives a normalized turbulent kinetic energy of 0.0136 and this agrees well with the measurement data. For the zero streamwise gradient condition, the value of β_i has to be changed according to equation (12) and the corresponding value is $\beta_i = 0.1263$ for the modified $k-\omega$ model. Regarding the eddy frequency, the profile based on equation (4) is chosen and modified according to equation (11) while the logarithmic velocity profile is employed at the inlet by equation (2), as in the previous wind turbine.

The average undisturbed velocity magnitude during the measurements at the hub – height of the turbine was 7.6m/s . Consequently, in this paper, to show the universality of the model, a value of 8.6m/s , as well as a lower velocity of 6.2m/s is employed. The thrust coefficient is 0.75 for a range of hub – height velocities from 7m/s to 10m/s and it increases to 0.78 for the 6.2m/s inlet velocity at the hub – height.

Figs. 8 and 9 show the computed normalized velocity and turbulence along the hub – height for both the velocity and turbulence inlets and the experimental data.

The velocity has a similar trend as in the previous investigated wind turbine. The velocity drops to half of the undisturbed value at a distance $2.5D$ downstream of the wind turbine and then it gradually increases, reaching 80% of the value of the undisturbed velocity at $8D$ downstream of the turbine. It is noticeable that the behavior of the computationally predicted velocity appears to be the same for both velocity inlet values. The model, like in the previous wind turbine, predicts the recovery of the velocity and turbulence kinetic energy with a very good accuracy as seen

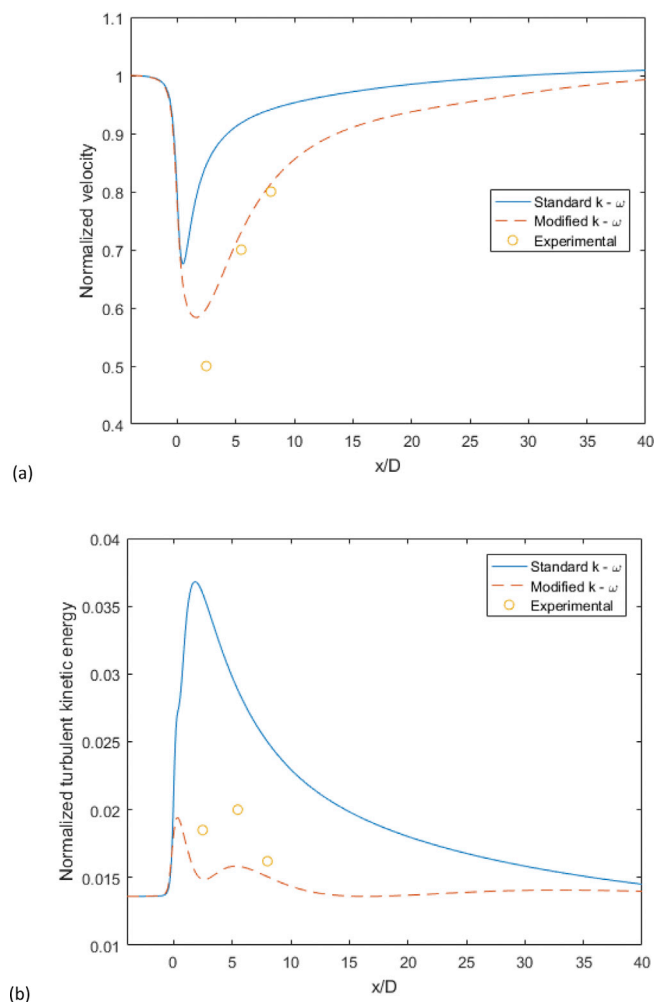


Fig. 8. (a) Normalized velocity and (b) turbulent kinetic energy along the streamwise direction at the hub – height for $U_{hub} = 8.6\text{m/s}$.

in Figs. 8 and 9, while the results are as good in the near wake region.

As far as the turbulent kinetic energy is concerned, a similar behavior with the Nibe turbine is illustrated. The maximum value does not appear in the near wake region but rather a few characteristic lengths away from the turbine, and this is not predicted by the model. However, in the far wake region the correct values of the turbulent kinetic energy are recovered and maintained along the domain until the outlet.

The small differences in the velocity and turbulent kinetic energy at the rear of the turbine between the 2 different inlet velocities are related to the very small difference in the thrust coefficient of the turbine. As shown in the Nibe wind turbine, the results are more reliable for high thrust coefficients. The same applies here for the Holec turbine but the differences are very small, especially for the velocity and this is due to the very small difference in the thrust coefficient. It is also noticeable again that the standard $k-\omega$ model failed to predict the velocity and the turbulent kinetic energy everywhere throughout the domain as expected.

Regarding the errors in the turbulent kinetic energy with the experimental data, although a significant improvement has been attained when compared with experimental data, the differences were generally high. These errors were of the order of magnitude of 20% for the case of 8.6m/s velocity at the hub – height at distances $2.5D$ and $5.5D$ downstream of the turbine while for the case of 6.2m/s velocity at the hub – height at the same distances, the error was less than 10%. In both velocity inlets, however, the turbulent kinetic energy at a distance $8D$ downstream of the turbine, the errors were approximately 2% and 6% for the 6.2m/s and 8.6m/s velocity inlet, respectively.

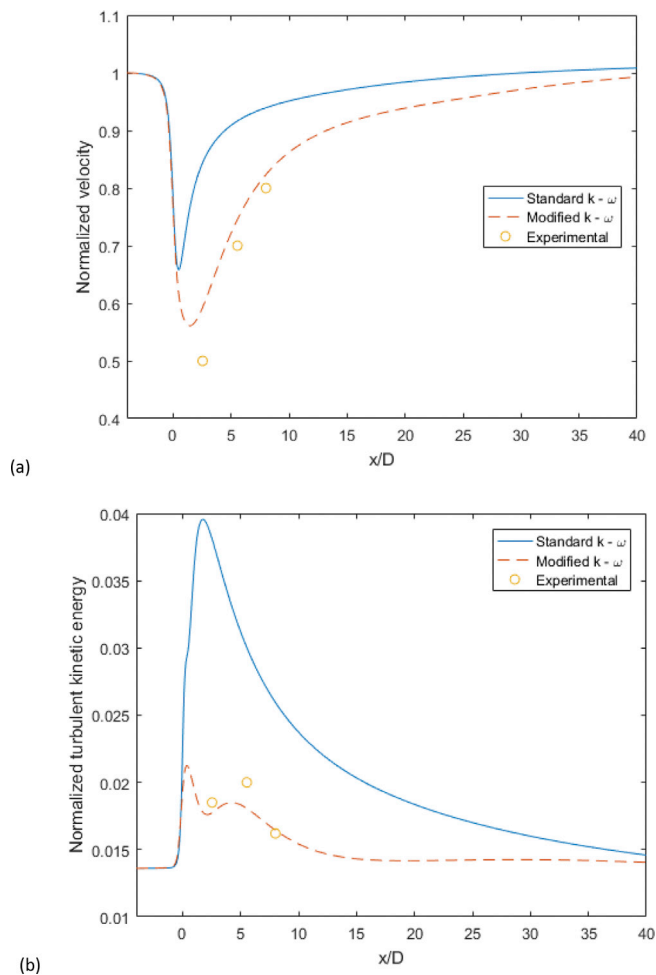


Fig. 9. (a) Normalized velocity, and (b) turbulent kinetic energy along the streamwise direction at the hub – height for $U_{hub} = 6.2\text{m/s}$.

Finally, regarding the errors in the velocity, as is the case of the Nibe turbine, the error in the velocity was approximately 20% in the near wake region, while in the far wake region it was about 6% or smaller regardless of the velocity inlet. In any case, for both turbines, for higher thrust coefficients, the results for both the velocity and turbulent kinetic energy were closer to the experimental data and far closer than the standard $k - \omega$ model.

In general, the modified $k - \omega$ model showed significant improvement when compared with the standard $k - \omega$ model which is of paramount importance, especially for wind farm simulations where the power output and possible future structural damage will be better predicted.

5. Conclusions

For wind farm simulations, using a steady RANS model, the recovery of the wind properties in the turbine wakes can affect the accurate prediction of the performance of the downstream turbine. In this paper, a modified $k - \omega$ model for simulating small wind turbine wakes for a uniform roughness flat terrain in a neutrally stratified atmospheric boundary layer is proposed. A condition for achieving the zero streamwise gradients for all flow variables has been mathematically produced. The model has been successfully implemented and tested in an empty domain for various turbulence levels and friction velocity values. The modified $k - \omega$ model has been employed for the simulation of 2 small wind turbines for different inlet conditions with the actuator disk model based on the thrust coefficient of the turbines. The comparison of the results in the near wake region for both wind turbines with available

experimental data was mediocre which may have been expected due to the very simplistic model that has been employed to represent the wind turbines. For higher thrust coefficients, the results were more accurate than for lower thrust coefficients for both the velocity and turbulent kinetic energy although the difference was small. In the far wake region, however, the comparison of the velocity and turbulence levels for both wind turbines with the experimental data was relatively good due to the imposition of the zero streamwise gradient condition for all variables. In all cases, the modified $k - \omega$ model produced results far closer to the experimental data rather than the standard $k - \omega$.

References

- Allaers, D., Meyers, J., 2015. Large eddy simulation of a large wind – turbine array in a conventionally neutral atmospheric boundary layer. *Phys. Fluids* 27, 065108. <https://doi.org/10.1063/1.4922339>.
- ANSYS FLUENT 14.0, 2011. Theory Guide. Release 14.0 @ ANSYS. Inc.
- Blocken, B., Stathopoulos, T., Carmeliet, J., 2007. CFD simulation of the atmospheric boundary layer: wall function problems. *Atmos. Environ.* 41 (2), 238–252.
- Cabezon, D., Hansen, K., Barthelmie, R.J., 2010. Analysis and validation of CFD wind farm models in complex terrain. Effects induced by topography and wind turbines. In: *EWEC2010*. Warsaw, Poland, pp. 1–4.
- Castellani, F., Vignaroli, A., 2013. An application of the actuator disc model for wind turbine wakes calculations. *Appl. Energy* 101, 432–440.
- Churchfield, M.J., Lee, S., Moriarty, P.J., Martinez, L.A., Leonardi, S., Vijayakumar, G., Brasseur, J.G., 2012a. A large – eddy – simulation of wind – plant aerodynamics: preprint. 21, pp., NREL Report No.CP-5000-53554. *J. Atmos. Ocean. Technol.* 27 (8), 1302–1317.
- Churchfield, M.J., Lee, S., Michalakes, J., Moriarty, P.J., 2012b. A numerical study of the effects of atmospheric and wake turbulence on wind turbine dynamics. *J. Turbul.* 13, N14. <https://doi.org/10.1080/14685248.2012.668191>.
- Cleijne, J.W., 1992. Results of Sexbierum Wind Farm Report MT-TNO Apeldoorn, pp. 92–388.
- Durbin, P.A., 1996. On the $k - \epsilon$ stagnation point anomaly. *Int. J. Heat Fluid Flow* 17 (1), 89–90, 1996.
- El – Askary, W.A., Sakr, I.M., Abdelsalam, A.M., Abuhegazy, M.R., 2017. Modeling of wind turbine wakes under thermally – stratified atmospheric boundary layer. *J. Wind Eng. Ind. Aerod.* 160, 1–15.
- Franke, J., Hellsten, A., Schlunzen, H., Carissimo, B., 2007. Best Practice Guideline for the CFD Simulation of Flows in the Urban Environment. COST Office, COSTAction732: Quality Assurance and Improvement of Microscale Meteorological Models.
- Goodfriend, E., Katopodes Chow, F., Vanella, M., Balaras, E., 2015. Improving large – eddy simulation of neutral boundary layer flow across grid interfaces. *Mon. Weather Rev.* 143, 3310.
- Hargreaves, D.M., Wright, N.G., 2007. On the use of the $k - \epsilon$ model in commercial CFD software to model the neutral atmospheric boundary layer. *J. Wind Eng. Ind. Aerod.* 95 (5), 355–369.
- Juretic, F., Kozmar, H., 2013. Computational modeling of the neutrally stratified atmospheric boundary layer flow using the standard $k - \epsilon$ turbulence model. *J. Wind Eng. Ind. Aerod.* 115, 112–120.
- Kasmi, A.E., Masson, C., 2008. An extended $k - \epsilon$ model for turbulent flow through horizontal – axis wind turbines. *J. Wind Eng. Ind. Aerod.* 96, 103–122.
- Makridis, A., Chick, J., 2013. Validation of a CFD model of wind turbine wakes with terrain effects. *J. Wind Eng. Ind. Aerod.* 123, 12–29.
- Menter, F.R., 1994. Two – equation eddy – viscosity turbulence models for engineering applications. *AIAA J.* vol. 32, 1598–1605.
- Mikkelsen, R., 2003. Actuator Disc Methods Applied to Wind Turbines. Ph.D. Thesis. Technical University of Denmark.
- Mokhtarzadeh – Dehghan, M.R., Akcayoglu, A., Robins, A.G., 2012. Numerical study and comparison with experiment of dispersion of a heavier – than – air gas in a simulated neutral atmospheric boundary layer. *J. Wind Eng. Ind. Aerod.* 110, 10–24.
- Nedjari, H.D., Guerri, O., Saighi, M., 2017. CFD wind turbines wake assessment in complex topography. *Energy Convers. Manag.* 138, 224–236.
- O’Sullivan, J.P., Archer, R.A., Flay, R.G.J., 2011. Consistent boundary conditions for flows within the atmospheric boundary layer. *J. Wind Eng. Ind. Aerod.* 99 (1), 65–77.
- Panofsky, H.A., Dutton, J.A., 1984. Atmospheric Turbulence. John Wiley & Sons Ltd, New York.
- Parente, A., Gorle, C., van Beeck, J., Benocci, C., 2011. Improved $k - \epsilon$ model and wall function formulation for the RANS simulation of ABL flows. *J. Wind Eng. Ind. Aerod.* 99, 267–278.
- Porte – Agel, F., Wu, Y., Lu, H., Conzemius, R., 2011. Large – eddy simulation of atmospheric boundary layer flow through wind turbines and wind farms. *J. Wind Eng. Ind. Aerod.* 99, 154–168.
- Prosathopoulos, J., Politis, E., Chaviaropoulos, P., Rados, K., Schepers, J., Cabezon, D., Hansen, K.S., Barthelmie, R., 2010. In: *CFD Modeling of Wind Farms in Flat and Complex Terrain*. EWEC 2010, Warsaw, Poland.
- Richards, P.J., Hoxey, R.P., 1993. Appropriate boundary conditions for computational wind engineering models using the $k - \epsilon$ turbulence model. *J. Wind Eng. Ind. Aerod.* 46 – 47, 145–153.
- Richards, P.J., Norris, S.E., 2015. Appropriate boundary conditions for a pressure driven boundary layer. *J. Wind Eng. Ind. Aerod.* 142, 43–52.

- Simisioglou, N., Karatsioris, M., Nilsson, K., Breton, S.P., Ivanell, S., January 2016. The actuator disc concept in PHOENICS. 13th deep sea offshore wind R&D conference. EERA DeepWind 2016 20–22 (Trondheim, Norway).
- Taylor, G.J., Milborrow, D.J., McIntosh, D.N., Swift-Hook, D.T., 1985. Wake measurements on the Nibewindmills. In: Proceedings of Seventh BWEA Wind Energy Conference, Oxford, pp. 67–73.
- Tominaga, Y., Mochida, A., Yoshie, R., Kataoka, H., Nozu, T., Yoshikawa, M., Shirasawa, T., 2008. ALJ guidelines for practical applications of CFD to pedestrian wind environment around buildings. *J. Wind Eng. Ind. Aerod.* 96, 1749–1761.
- Wilcox, D., 1988. Reassessment of the scale – determining equation for advanced turbulence models. *AIAA J.* 26 (11), 1299–1310.
- Wilcox, D., 2006. *Turbulence Modeling for CFD*, third ed. DCW Industries, Inc.
- Yan, B.W., Li, Q.S., He, Y.C., Chan, P.W., 2016. RANS simulation of neutral atmospheric boundary layer flows over complex terrain by proper imposition of boundary conditions and modification on the $k - \epsilon$ model. *Environ. Fluid Mech.* 16, 1–23. <https://doi.org/10.1007/s10652-015-9408-1>.
- Yang, Y., Gu, M., Chen, S., Jin, X., 2009. New inflow boundary conditions for modeling the neutral equilibrium atmospheric boundary layer in computational wind engineering. *J. Wind Eng. Ind. Aerod.* 97, 88–95.